Talbot Coupling of an array of quantum cascade lasers

F. Grillot[a,b], A. Gavrielides[b], O. Spitz[a,d], T. C. Newell[c], and M. Carras[d]

[a]LTCI, Télécom ParisTech, Université Paris-Saclay, 46 rue Barrault, Paris, France
[b]Center for High Technology Materials, University of New-Mexico, Albuquerque, NM USA
[c]Air Force Research Laboratory, Directed Energy Directorate, 3550 Aberdeen Avenue SE, Albuquerque, NM USA
[d]mirSense, Centre d'intégration NanoInnov, 8 avenue de la Vauve, Palaiseau, France

ABSTRACT

Quantum cascade lasers (QCL) are semiconductor lasers based on ultrafast intersubband transitions with picosecond timescale that have become the most suitable laser sources from the mid-infrared to the THz range, due to their compactness, efficiency and high room temperature performances. In particular, high-power QCLs are powerful sources for optical countermeasures, including night vision blinding and missile out steering. This work investigates the nonlinear dynamical features of coupling of linear arrays of emitters in the so-called Talbot configuration for phase-locking operation using broad area emitters. These initial results are of paramount importance for creating future bright infrared sources with Watt-level power.

Keywords: Quantum cascade lasers, Talbot cavity, high power lasers

1. INTRODUCTION

High-power quantum cascade lasers (QCLs) are powerful sources for optical countermeasures, including night vision blinding and missile out steering.[1] In order to increase the power, several solutions have been proposed such as using external optical feedback, which has been shown to be an efficient technique to control the beam quality and dynamical stability, without resorting to integrated solutions.[2] This paper aims at investigating the coupling of linear arrays of emitters in the Talbot configuration based external cavity. Talbot effect is a well-known lensless optical phenomenon that the intensity pattern of an array of coherent emitters reproduces itself after a specific distance of propagation.[3–5] This effect has been exploited to phase-lock lasers in the near-infrared, which is called diffraction coupling scheme phase-locked array.[6] In the past, Talbot arrays have been investigated using single transverse mode diode laser arrays but not QCLs except in two very recent papers in which phase-locking using broad area emitters is unveiled.[7,8] In this paper, we investigate both theoretically and experimentally the complex dynamics arising in an array of QCLs.[9] We provide a comprehensive analysis of the Talbot cavity and show the existence of distinct regions depending on whether all the lasers are locked to the same frequency. Impact of the external cavity length and detuning between lasers is discussed. The results are promising for creating a bright infrared source with Watt-level power.

2. SINGLE MODE QCL COUPLED BY THE TALBOT EFFECT

The setup consists in an array of N QCLs placed side by side with a center-to-center distance d. The facet of the QCLs are cleaved on both sides so that emission occurs on both sides. On one side, the global emission properties of the array can be studied with that specific configuration. On the other side, a mirror is placed at a multiple of $\frac{Z_t}{8}$, with Z_t being the Talbot distance and scaling as $\frac{2nd^2}{\lambda}$. λ is the emission wavelength of the QCL and n is the refractive index of the medium between the QCLs array and the mirror. For instance, if the mirror is set at a distance equal to $\frac{Z_t}{8}$ as shown on Fig. 1, the pattern derived from the Talbot effect that is found at a distance $\frac{Z_t}{4}$ is back reflected to the array. This induces a coupling which can improve the emission properties of the linear QCL array in particular for creating a bright infrared source with Watt-level power.

Further author information: (Send correspondence to F.G.)
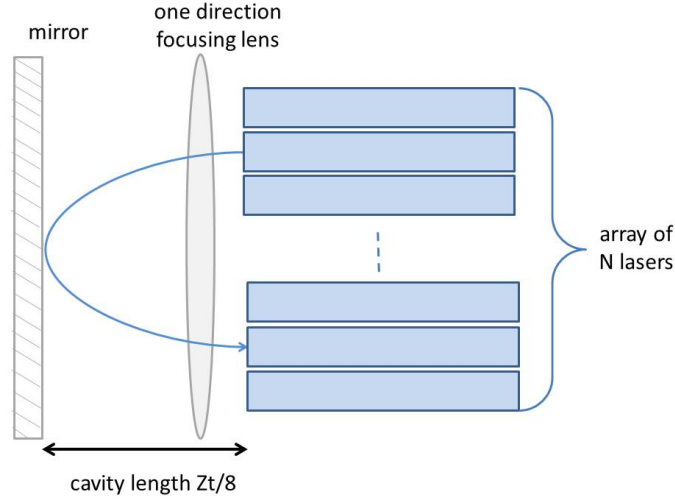F.G.: E-mail: frederic.grillot@telecom-paristech.fr

Figure 1. Schematic of the experimental setup when an array of N lasers is considered. In that case, the length of the Talbot cavity is set to $\frac{Z_t}{8}$ and therefore the image at $\frac{Z_t}{4}$ is sent back to the array.

The model that contains the essential features of coupling N QCLs grown on a chip consists of N equations for the field and $2N$ equations for the carriers,[10]

$$\frac{dE_n}{dt} = i\delta_n E_n + (1+i\alpha)N_n E_n + \eta \sum_{m=1}^{N} R_{nm}(\tau)E_m(t-\tau), \tag{1}$$

$$\frac{dZ_n}{dt} = \gamma_1[P + \gamma_3 V_n - \gamma_4 Z_n - (1+2Z_n)|E_n|^2], \tag{2}$$

$$\frac{dV_n}{dt} = \gamma_2[2Z_n - V_n + (1+2Z_n)|E_n|^2], \tag{3}$$

where the time t is measured in units of photon lifetime τ_p. The parameters γ_i for i between 1 and 4, and P, which are the normalized dimensionless parameters, are defined as follows in terms of the physical parameters of the QCLs:

$$\gamma_1 = \frac{\tau_P}{\tau_{32}}, \tag{4}$$

$$\gamma_2 = \left(\frac{\tau_{32}}{\tau_{21}} - 1\right)\frac{\tau_P}{\tau_{32}}, \tag{5}$$

$$\gamma_3 = \left(\frac{\tau_{32}}{2\tau_{21}} - 1 - \frac{\tau_{32}}{2\tau_{31}}\right)\frac{1}{\left(\frac{\tau_{32}}{\tau_{21}} - 1\right)}, \tag{6}$$

$$\gamma_4 = 2\left(1 + \frac{\tau_{32}}{2\tau_{31}}\right), \tag{7}$$

$$P \equiv \frac{N_p g \tau_P \tau_{32}}{2}\left(\frac{I_{in} - I_{th}}{q}\right), \tag{8}$$

Table 1. Experimental parameters as estimated or measured and published in various publications

References	11	12	13	14
γ_1	2.75	1.85	15.59/15.02	0.67/0.67
γ_2	16.49	10.48	90.56/55.77	4.1/0.17
γ_3	0.35	0.34	0.41/0.37	0.42/1.5
γ_4	2.81	2.82	2/2	2/2

Also, δ_n is the relative detuning from the frequency of a selected reference laser, for instance laser 1 is related to $\delta_1 = 0$. The coupling coefficients $R_{nm}(\tau)$ are obtained from the specific geometry of feedback as determined from the Talbot cavity or of the Fourier Transform cavity configuration. For example, in the case of a Talbot cavity, the coefficients $R_{nm}(\tau)$ are given using the approximations in Ref. 9 such as

$$R_{nm}(\tau) = \frac{e^{i\omega\tau}}{1 + \frac{i\tau}{2\tau_0}} \exp\left[i\frac{\pi}{2}(n-m)^2\frac{\tau_t}{\tau}\right] \qquad (9)$$

where τ is the roundtrip time of the external coupling path, $\tau_0 = \frac{\omega a^2}{2c^2 t_p}$ is related to the waist a, or the aperture of the lasers of the radiation emitted by each QCL in normalized time units, and $\tau_t = \frac{\omega d^2}{\pi c^2 t_p}$ is the Talbot distance expressed in normalized time units.

The coefficients δ_n are the detunings of the fundamental uncoupled frequency from laser No. 1. We then estimate that the detunings will be random to within $\delta\nu$ the HWHM of the gain of the QCLs if the lengths of the cavities are random. The initial computations will assume that the detunings are equal to zero since we expect that the QCLs will be grown on the same substrate.

For an order parameter i.e. an estimate of the coherence between the lasers is:

$$r(t) = \frac{1}{N}\frac{< |\sum_{n=1}^{N} E_n(t)|^2 >}{< \sum_{n=1}^{N} |E_n(t)|^2 >}, \qquad (10)$$

which is inversely proportional to the beam quality as it can be determined from the near field and far field data. $E_n(t)$ is the field from each laser in the array. The order parameter $r(t)$ can be consider as an interference term of several fields. For equal phases, r converges towards the unity while for anti-phase or random phases it leads to 0. This is the same effect in the far field except the overall envelope is the Fourier transform hence on the axis one either get $r \to 1$ for equal phases or $r \to 0$ for random or anti-phase. In general we would like to monitor the time development of the $r(t)$ order parameter in time to identify any possible global bifurcations.

3. NUMERICAL RESULTS FOR Z_T

3.1 Effects of the detuning

In this section we will try to understand the effects of the detuning between the lasers. We assume that either due to the manufacture or due to thermal effects there may be imperfections in the lengths of the individual cavities that may lead to the possibility that the laser will not operate on the same frequency, thus introducing detuning to the array. This effect was included in the model equations Eq.(1)-(3). To examine this more carefully we would like to recast the Eq.(1)-(3) so that the frequency of the individual laser $\omega_n = \Omega_n \tau_p$ is included explicitly:

$$\frac{dE_n}{dt} = i\omega_n E_n + (1 + i\alpha)N_n E_n + \eta \sum_{m=1}^{N} R_{nm}(\tau)E_m(t-\tau), \qquad (11)$$

We will only need at this time the equations for the fields as the equations for the populations will be unchanged. We can then define the average frequency of the N lasers collection by

$$\omega_0 = <\omega_n> = \frac{1}{N} \sum_{n=1}^{N} \omega_n, \tag{12}$$

We then redefine the field as $A_n = e^{-i\omega_0 t} E_n$ and obtain

$$\frac{dA_n}{dt} = i\delta_n A_n + (1 + i\alpha) N_n A_n + \eta e^{-i\omega_0 \tau} \sum_{m=1}^{N} R_{nm}(\tau) A_m(t - \tau), \tag{13}$$

We can eventually regard δ_n as random numbers with zero mean on an interval of $(-D, D)$ with probability $P(\delta) = 1/2D$. Similarly, we will restrict $\omega_0 \tau$ on the interval of $(-\pi, \pi)$ under symmetry considerations. In Fig. 2, we compute the order parameter as a function of time for two values of mean square deviation of the detuning. It is obvious that as the correlation increases, the order parameter decreases and at a value close to 0.1004 the locking is broken and the lasers are operating at their own frequencies. To obtain an idea of the actual physical detuning required to break locking we find that if $\lambda = 5\mu m$, and the cavity lifetime is of the order of the picosecond, then the RMS of $\Delta\nu = 7GHz$ corresponds to the correlation of $\sqrt{0.1004}$.
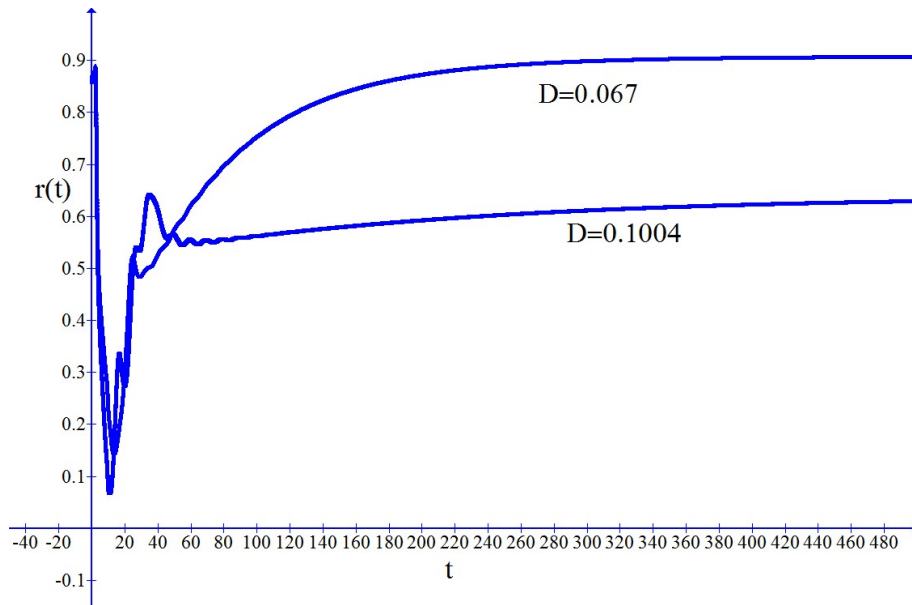

Figure 2. Order parameter $r(t)$ as a function of time for two mean square deviations of the detuning, $\sigma^2 = 0.1004$ and $\sigma^2 = 0.067$.

3.2 Numerical results for $\frac{z_t}{4}$

We will examine a set of seven QCLs coupled by the Talbot effect in which the external cavity is set at $2L = \frac{z_t}{4}$. The coupling phases are symmetric and approximately equal to each other. In the notation introduced earlier the pumping is assumed to be $P=2.0$, the enhancement factor $\alpha = 2$ with a fill factor of $f = 0.1$.

In Fig. 3 we show the bifurcation of amplitude and frequency of laser 1 as well as of the order parameter as a function of the feedback η. Three distinct regions are apparent immediately. In the first region it is clear that the laser is not at a steady state for values of $\eta \leq 0.17$. An example of the time dependence of the order parameter in this region for a value of $\eta = 0.05$ is shown in Fig. 4. It is clear that it is oscillating at a small frequency and the numerical calculation indicates that the frequencies of the lasers are not locked and not related to each other as well as the laser amplitudes. For the region of $\eta \geq 0.17$ and $\eta \leq 0.62$ all three variables indicated in Fig. 3 are constant and therefore the lasers are in an in-phase steady state and therefore the order parameter approaches
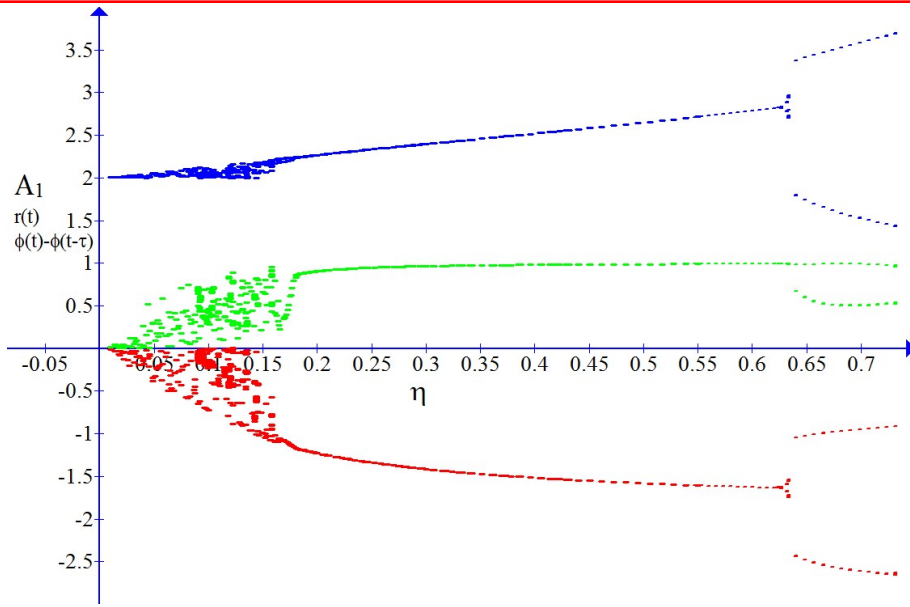
Figure 3. Amplitude of the laser 1 A_1 (blue scatter plot), r(t) (green scatter plot), and frequency shift due to the external cavity $\phi_1(t) - \phi_1(t - \tau)$ (red scatter plot) as a function of feedback strength η.

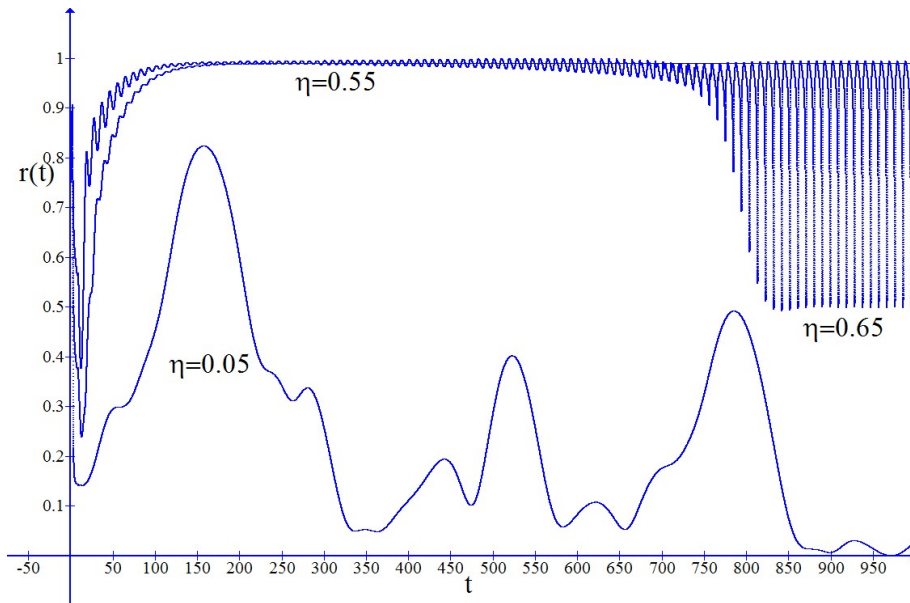
Figure 4. Bifurcation using the order parameter $r(t)$ as a function of η.

1. All the lasers are locked to the same frequency and it develops as a function of η in the usual manner as in single lasers with an external cavity. The order parameter for $\eta = 0.55$ is shown in Fig. 4 and is flat at $r=0.988$ once the transients have died down. Finally, in the third region $\eta \geq 0.62$ we find regular pulsations. In particular we show in Fig. 4 for $\eta = 0.65$ the time development of the order parameter. It is clear that the lasers show a mode-locked behavior since each laser lase at its own frequency and with relative phases equal to zero or in a in-phase condition. In addition, the frequencies as well as the amplitudes obey.

$$S_n = S_{N-n+1} \,, \tag{14}$$

where S stands for either A or $\omega\tau$. We have only a preliminary glimpse in this region but it appears that this may have interesting properties for mode-locking applications, in particular as the number of lasers in a bar becomes rather large.

4. EXPERIMENTS

As a precursor to the Talbot cavity array phasing we initially investigate a broad-area QCL (BA-QCL) subject to external cavity feedback. The motivation for this first step comes in part from the behavior of BA-QCLs. These often exhibit lasing on one principal transverse mode[15] with other transverse modes strongly suppressed. The importance to the Talbot cavity is that each emitter in the array may not have to be constrained for the fundamental transverse mode. With BA-QCLs lasing on a single mode and with Talbot feedback selecting a supermode, then we may be able to widen each emitter so as to increase the gain and total output power while remaining in the fundamental supermode. As a test of feedback we place a 40 μm wide, 3 mm long, λ=4.7 μm QCL in an external cavity, see Fig. 5 which is a schematic of the external cavity (ECL) experimental arrangement. The ECL is bounded by the QCL and rotatable partially reflective mirror (PR). The components consist of a f=1.87 mm collimating lens (CL), pellicle beam splitter with low reflectivity at 4.7 μm (BS), a midinfrared polarizer to vary the feedback intensity (P), f=200 mm focusing lens (FL), integrating sphere and detector (PM), an amplified Mercury-Cadmium-Telluride (MCT) detector, mirrors (M) and Spectral Products DK240 monochromator. The primary component is the mirror that is rotated to create different cavity modes, thus steering the beam or inciting various dynamical effects.
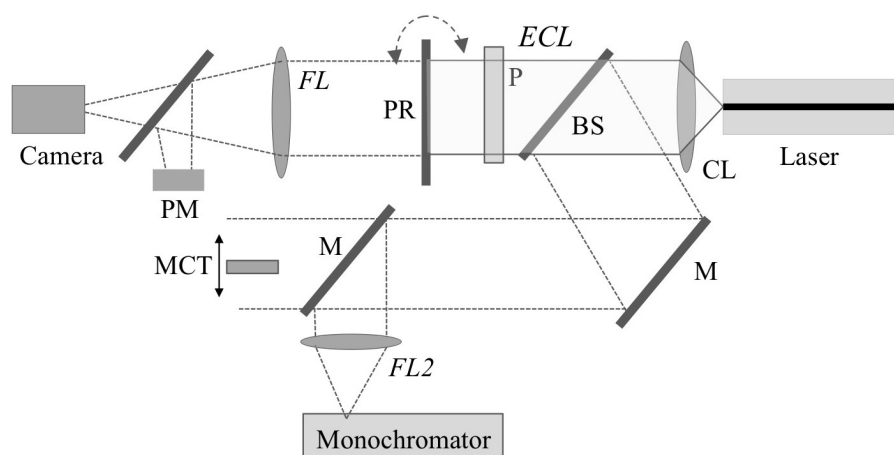

Figure 5. Schematic of experimental arrangement

Near-field images at the facet are obtained using the CL and FL lens pair magnifying the image onto a Xenics Onca 3369 InSb camera. From the camera image a line scan is extracted. In Fig. 6, (a) and (b) show the near field intensity plotted versus the position on the laser facet. Figure 6(c) shows the light-current curves for the two cases. Fig. 6 (a) is the free-running case. A principal M=9 mode is observed although the intensity of each antimode varies and the furthest to the right is quite dim. In the far-field, two peaks are observed at angles 33 degrees as predicted although other lesser peaks are also observed. This image is not normally observed in diode counterparts that would show an irregular flat-top peak indicative of many transverse modes along with filamentation. Fig. 6 (b) is taken with feedback. In this case the created mode shows one dominant peak in the near-field. While it is not the fundamental mode of the BA-QCL, it does show that distinct modes can be created with feedback. The light-current curves in Fig. 6 (c) are measured from a sampling of the light and show that the feedback improves the threshold current while also increasing the modal gain. Note that the total power emitted at the facet is much higher. The significant result that may be applied to the Talbot question, suggests that the emitter width may be widened with the array maintaining coherent phase-locking. However

we note that the created mode is highly mirror angle dependent. Curious modes are created and destroyed as the mirror is rotated. Furthermore, these modes can compete showing temporal oscillations.
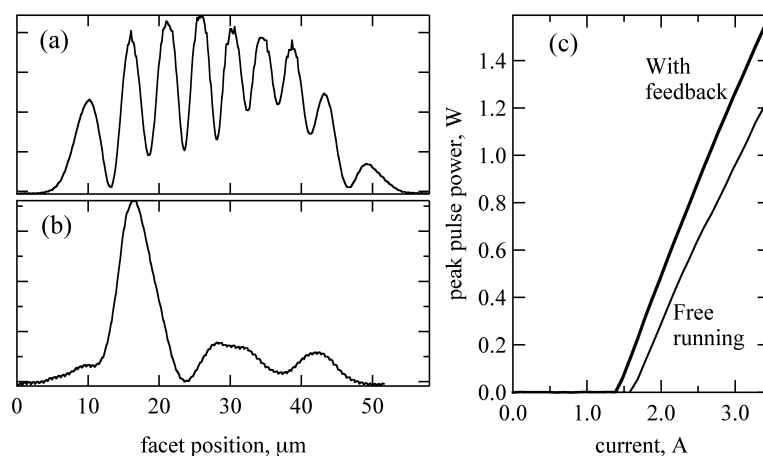

Figure 6. (a) Line scan from near-field facet image for the free-running case and (b) feedback forcing single peak mode. (c) Light-current curves for the free-running and single peak feedback case.

5. CONCLUSIONS

This paper gives initial theoretical results on the nonlinear dynamical features of coupling of linear arrays of emitters in the Talbot configuration for phase-locking operation. We provide a comprehensive analysis of the Talbot cavity and show the existence of distinct regions depending on whether all the lasers are locked to the same frequency. These initial results are of paramount importance for creating future bright infrared sources with Watt-level power.

Acknowledgments

REFERENCES

[1] Faist, J., [*Quantum Cascade Lasers*], Oxford University Press (2013).
[2] Ferré, S., Jumpertz, L., Carras, M., Ferreira, R., and Grillot, F., "Beam shaping in high-power broad-area quantum cascade lasers using optical feedback," *Nature Scientific Reports* **7** (2017).
[3] Talbot, H. F., "Facts relating to the optical science," *Philos. Mag.* **9** (1836).
[4] Lord Rayleigh, "On copying diffraction gratings and on some phenomenon connected therewith," *Philos. Mag.* **11** (1881).
[5] Wen, J. M., Zhang, Y., and Xiao, M., "The Talbot effect: recent advances in classical optics, nonlinear optics, and quantum optics," *Adv. Opt. Photon.* **5** (2013).
[6] Evans, G. A. and Hammer, J. M., [*Surface Emitting Semiconductor Lasers and Arrays*], Academic Press, INC., San Diego (1993).
[7] Wang, L., Zhang, J., Jia, Z., Zhao, Y., Liu, C., Liu, Y., Zhai, S., Ning, Z., Xu, X., and Liu, F., "Phase-locked array of quantum cascade lasers with an integrated talbot cavity," *Opt. Express* **24**, 30275–30281 (2016).
[8] Meng, B., Qiang, B., Rodriguez, E., Hu, X. N., Liang, G., and Wang, Q. J., "Coherent emission from integrated Talbot-cavity quantum cascade lasers," *Opt. Express* **25**, 3077–3082 (2017).
[9] Peterson, P., Gavrielides, A., and Siodeharma, M. P., "Extraction characteristics of a one dimensional Talbot cavity with stochastic propagation phase," *Opt. Express* **8** (2001).

[10] Erneux, T., Kovanis, V., and Gavrielides, A., "Nonlinear dynamics of an injected quantum cascade laser," *Phys. Rev. E* **88**, 032907 (2013).

[11] Gentsy, T., Elsässer, W., and Mann, C., "Intensity noise properties of quantum cascade lasers," *Opt. Express* **13**, 2032–2039 (2005).

[12] Petitjean, Y., Destic, F., Mollier, J. C., and Sirtori, C., "Dynamic modeling of terahertz quantum cascade lasers," *J. Select. Topics in Quant. Electr.* **17**, 22–29 (2011).

[13] Meng, B. and Wang, Q. J., "Theoretical investigation of injection-locked high modulation bandwidth quantum cascade lasers," *Opt. Express* **20**, 1450–1464 (2012).

[14] Wang, C., Grillot, F., Kovanis, V., and Even, J., "Investigation of injection-locked quantum cascade lasers based on rate equations," *J. Appl. Phys.* (2013).

[15] Bai, Y., Slivken, S., Darvish, S. R., Haddadi, A., Gokden, B., and Razeghi, M., "High power broad area quantum cascade lasers," *Appl. Phys. Lett.* **95** (2004).